

Trivalent Aluminum Ion Conducting Characteristics in $\text{Al}_2(\text{WO}_4)_3$ Single Crystals

N. Imanaka, S. Tamura, M. Hiraiwa, and G. Adachi*

Department of Applied Chemistry, Faculty of Engineering, Osaka University, 2-1 Yamadaoka, Suita, Osaka, 565-0871 Japan

H. Dabkowska, A. Dabkowski, and J. E. Greedan

Brockhouse Institute for Materials Research, 1280 Main Street West, Hamilton, Ontario, Canada, L8S 4M1

Received April 24, 1998. Revised Manuscript Received July 13, 1998

Single crystals of the trivalent Al^{3+} ion conductor $\text{Al}_2(\text{WO}_4)_3$ were grown by the Czochralski (CZ) method. The ionic conductivity in the a -, b -, and c -axis directions was determined and Al^{3+} ion conduction in the direction of the b -axis was concluded to be the most suitable pathway for ion migration in the tungstate grains. The ionic conductivities in the a - and c -axis directions were 0.3 and 10^{-2} times lower than the conductivity in the b -axis. Consistent with this observation, the lowest activation energy (E_a) for Al^{3+} ion migration was obtained for the b -axis direction. The E_a of the conductivity in the direction of the c -axis was almost comparable to that of the polycrystalline samples and the E_a of the Al^{3+} ionic conduction in the grains of this material was explicitly verified to be controlled by the Al^{3+} ionic migration in the c -axis direction. The Al^{3+} ion conductivity of the polycrystalline sample was higher in the higher temperature region, indicating that the conductivity in the grain boundaries enhances the total Al^{3+} ion conductivity to a considerable extent. From the oxygen pressure dependencies of the electrical conductivity and the polarization behavior, the single crystals were demonstrated to be pure Al^{3+} ionic conductors showing an anisotropic ion conducting behavior.

1. Introduction

Solid electrolytes in which macroscopic ion migration predominantly occurs are of great interest for application in chemical sensors and electrochemical power-generating cells for heart pacemakers, for example. Typically, the migrating ions in solid electrolytes have been limited mono- or divalent ions. In a few cases, trivalent cation conduction has been claimed for such materials as Ln^{3+} - β'' -alumina,^{1–8} β - LaNb_3O_9 ,⁹ $\text{LaAl}_{11}\text{O}_{18}$,¹⁰ and $\text{LaAl}_{12}\text{O}_{18}\text{N}$.¹⁰ However, no clear and direct demonstration of specific trivalent ion conduction in these solids has been accomplished.

Recently, trivalent ion conduction in solids has been directly demonstrated.^{11–13} The typical ionic species are aluminum and rare earth ions such as Sc, Y, and Er.

The crystal structure for the trivalent ion conductors is the $\text{Sc}_2(\text{WO}_4)_3$ type^{14–18} with orthorhombic symmetry. This tungstate has a quasilayered structure and the trivalent ions are positioned between the layers and migrate smoothly in the interlayer space. However, the tungstates investigated so far have been polycrystalline materials because of the difficulty in growing single crystals. In the polycrystals, there exist not only grains but also grain boundaries with pores, and the grain boundaries influence the ionic conducting characteristics to a considerable extent. Therefore, it is quite difficult to clarify the detailed pathway of the ionic conduction in the polycrystalline tungstate grains and, especially, to determine the preferred ionic migration direction with respect to the crystallographic axes. In our previous paper,¹³ we have directly and quantitatively demonstrated Al^{3+} ion conduction in polycrystalline $\text{Al}_2(\text{WO}_4)_3$. Previously, $\text{Al}_2(\text{WO}_4)_3$ single crystals were grown by the flux method from $\text{Na}_2\text{W}_2\text{O}_7$.¹⁹ The flux grown single

(1) Dunn, B.; Farrington, G. C. *Solid State Ionics* **1983**, 9 & 10, 223.

(2) Carrillo-Cabrera, W.; Thomas, J. O.; Farrington, G. C. *Solid State Ionics* **1983**, 9 & 10, 245.

(3) Ghosal, B.; Mangle, E. A.; Topp, M. R.; Dunn, B.; Farrington, G. C. *Solid State Ionics* **1983**, 9 & 10, 273.

(4) Farrington, G. C.; Dunn, B.; Thomas, J. O. *Appl. Phys.* **1983**, A32, 159.

(5) Dedecke, T.; Köhler, J.; Tietz, F.; Urland, W. *Eur. J. Solid State Inorg. Chem.* **1996**, 33, 185.

(6) Köhler, J.; Urland, W. *Solid State Ionics* **1996**, 86–88, 93.

(7) Köhler, J.; Balzer-Jöllenbeck, G.; Urland, W. *J. Solid State Chem.* **1996**, 122, 315.

(8) Köhler, J.; Urland, W. *Angew. Chem., Int. Ed. Engl.* **1997**, 36, 85.

(9) George, A. M.; Virkar, A. N. *J. Phys. Chem. Solids* **1988**, 49, 743.

(10) Warner, T. E.; Fray, D. J.; Davies, A. *Solid State Ionics* **1996**, 92, 99.

(11) Imanaka, N.; Kobayashi, Y.; Adachi, G. *Chem. Lett.* **1995**, 433.

(12) Imanaka, N.; Adachi, G. *J. Alloys Compd.* **1997**, 250, 492.

(13) Kobayashi, Y.; Egawa, T.; Tamura, S.; Imanaka, N.; Adachi, G. *Chem. Mater.* **1997**, 9, 1649.

(14) Abrahams, S. C.; Bernstein, J. L. *J. Chem. Phys.* **1966**, 45, 2745.

(15) Nassau, K.; Levinstein, H. J.; Loiacono, G. M. *J. Phys. Chem. Solids* **1965**, 26, 1805.

(16) Borchardt, H. J. *J. Chem. Phys.* **1963**, 39, 504.

(17) Nassau, K.; Shiever, J. W.; Keve, E. T. *J. Solid State Chem.* **1971**, 3, 411.

(18) Rode, E. Y.; Lysanova, G. V.; Kuznetsov, V. G.; Gokhman, L. Z. *Russ. J. Inorg. Chem.* **1968**, 13, 678.

crystals were approximately $3 \times 3 \times 1 \text{ mm}^3$, too small to measure the electrical conductivity in each direction. In addition, Na^+ ion, which is a well-known mobile ionic species in solid electrolytes, is included in the flux and can be easily speculated to function as a contaminant and to strongly affect the ionic conducting characteristics of the flux grown crystals.

Recently, we have succeeded in growing high-quality single crystals of $\text{Al}_2(\text{WO}_4)_3$.²⁰ Here, the modified Czochralski (CZ) method was applied to grow large single crystals without any contamination from a flux. The aim of this paper is to clarify the conducting characteristics of the Al^{3+} ion in $\text{Al}_2(\text{WO}_4)_3$ by using tungstate single crystals and to characterize the Al^{3+} ion conduction anisotropy.

2. Experimental Section

$\text{Al}_2(\text{WO}_4)_3$ single crystals were grown from reagent grade Al_2O_3 (99.9%) and WO_3 (99.9%) by the Czochralski method. The detailed procedure for single-crystal growth is described elsewhere.²⁰ The axis directions and lattice parameters of the single crystal were determined using a four-circle single-crystal diffractometer. The single crystals were cut into the shape of cylinders (thickness c.a. 0.6 mm) with the cylinder axes parallel to the a -, b -, and c -axes.

Pt electrodes were sputtered on both center surfaces (0.62 cm in diameter) of the sample pellets. The ac electrical conductivity (σ_{ac}) of the pellets was measured by a complex impedance method in the frequency range between 20 Hz and 1 MHz (Precision LCR meter 8284A, Hewlett-Packard) in the temperature range from 300 to 600 °C.

The voltage which appeared by passing a constant current (0.1 μA) through the pellet with the two Pt electrodes was monitored as function of the time. The dc conductivity (σ_{dc}) was calculated by the current passed, the steady-state voltage generated, the surface area (diameter 0.62 cm) of the Pt electrode, and the thickness of the pellet. The polarization behavior was investigated by measuring the time dependencies of the σ_{dc}/σ_{ac} ratio.

The oxygen pressure variation of the electrical conductivity for the single crystals was measured under various oxygen pressures, such as pure oxygen ($P_{\text{O}_2} = 1 \times 10^5 \text{ Pa}$), nitrogen ($P_{\text{O}_2} = 2 \times 10 \text{ Pa}$), helium ($P_{\text{O}_2} = 4 \text{ Pa}$), and a CO-CO₂ buffer gas atmosphere ($P_{\text{O}_2} = 10^{-12}$ – 10^{-18} Pa).

Electrolysis of the single crystal was carried out by applying 10 V at 900 °C for 400 h in an air atmosphere to identify the migrating ionic species in the crystal.

3. Results and Discussion

3.1. The Characterization of the $\text{Al}_2(\text{WO}_4)_3$ Single Crystals. Figure 1 shows one of the representative single crystals grown by the CZ method. Highly transparent single crystals were obtained and the high quality of the crystals was verified by use of a polarizing microscope. The powder obtained by pulverizing a single crystal was found to be identical to the polycrystalline $\text{Al}_2(\text{WO}_4)_3$ powder by X-ray powder diffraction analysis.

From measurements on the four-circle diffractometer, the lattice parameters of the single crystals were precisely determined to be $a = 1.2493 \text{ nm}$, $b = 0.9045 \text{ nm}$, $c = 0.9092 \text{ nm}$, with orthorhombic symmetry, in excellent agreement with the ones obtained from the $\text{Al}_2(\text{WO}_4)_3$ polycrystals²¹ ($a = 1.2574 \text{ nm}$, $b = 0.9045 \text{ nm}$,

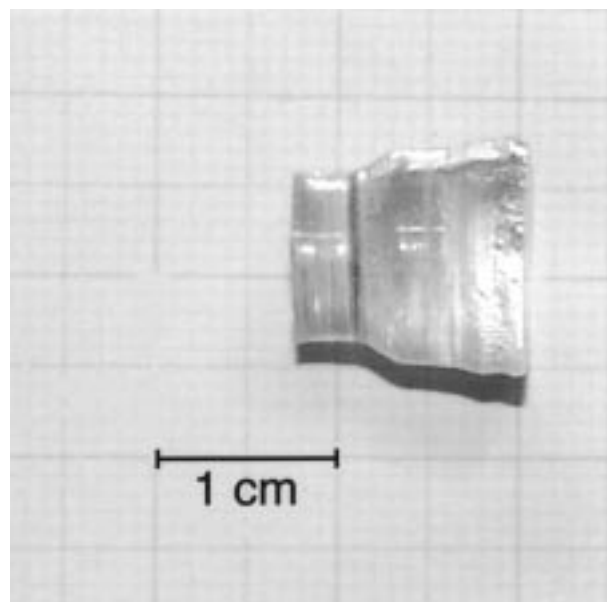


Figure 1. One of the representative single crystals grown by the CZ method.

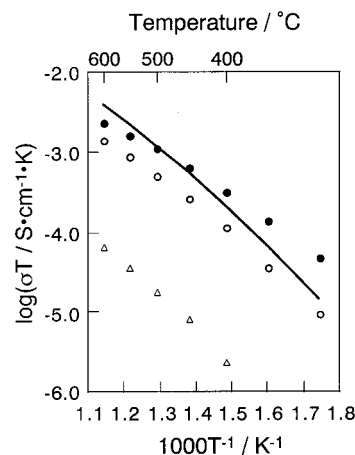


Figure 2. The electrical conducting properties toward each axis direction for the $\text{Al}_2(\text{WO}_4)_3$ single crystal: \circ , a -axis; \bullet , b -axis; \triangle , c -axis; solid line, polycrystal.

$c = 0.9121 \text{ nm}$). The direction of the single-crystal growth was determined to be parallel to the b -axis.

3.2. Electrical Conducting Characteristics. The electrical conductivities parallel to the a -, b -, and c -axis directions were measured for the $\text{Al}_2(\text{WO}_4)_3$ single crystal and are presented in Figure 2.

Among the three directions, the conductivity along the b -axis shows the highest value and the conductivity at temperatures below 500 °C is higher than that of polycrystalline $\text{Al}_2(\text{WO}_4)_3$ (solid line). At temperatures higher than 500 °C, the b -axis conductivity is almost comparable and becomes lower than the value for the polycrystalline samples at 600 °C. The a -axis conductivity was $3/5$ of that for the b -axis at higher temperatures, while the values at low temperatures are almost equivalent. The c -axis conductivity is 2 orders of magnitude lower than that of the polycrystalline sample. The activation energies (E_a) for ionic migration in the tungstate solids were 63.5, 48.2, and 73.7 kJ/mol for the a -, b -, and c -axis directions, respectively, while the E_a

(19) Petermann, K.; Mitzscherlich, P. *IEEE J. Quantum Elec.* **1987**, *QE-23*, 1122.

(20) Dabkowska, H.; Dabkowski, A.; Greedan, J. E.; Tamura, S.; Hiraiwa, M.; Imanaka, N.; Adachi, G. *J. Cryst. Growth* in press.

(21) De Boer, J. J. *Acta Crystallogr.* **1974**, *B30*, 1878.

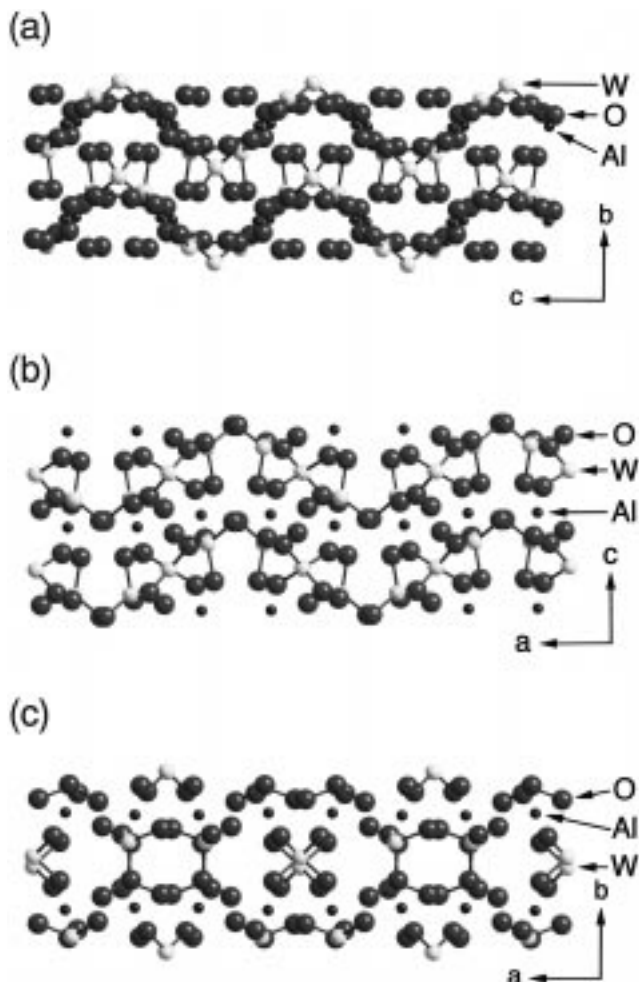


Figure 3. The $\text{Al}_2(\text{WO}_4)_3$ crystal model viewed from each axis direction: (a) a -axis, (b) b -axis, and (c) c -axis.

value of the polycrystalline sample is around 70.6 kJ/mol. Comparison shows that the E_a values of the polycrystalline sample are nearly the same as for the c -axis. This is because the orientation of the grains is randomly distributed in the polycrystalline samples, and thus, the pathway for ion migration which has the highest E_a value determines that for the polycrystalline case. Since the E_a values for the a - and b -axes are much lower than that for the c -axis, the slopes of the curve for a - and b -axes in the $\log(\sigma T) - 1/T$ relation show a gentler curvature. Figure 3a–c shows the crystal structure viewed from each axis direction and can be used to understand the experimental results. For example, although large voids exist along a , the Al^{3+} ions do not occupy the space. For the b - and c -directions, the Al^{3+} ions are in interlayer positions. However, the interlayer spacing is more narrow normal to the c -axis than the b -axis, which helps to explain the more facile ion migration pathway in the latter direction.

The oxygen pressure dependencies of the electrical conductivity for the single crystal along the a -, b -, and c -axis directions were carried out in the P_{O_2} range from 10^{-18} Pa to 10^5 Pa and are depicted in Figure 4. In the whole pressure region examined, the conductivity was almost constant in each axis direction. This phenomenon clearly indicates that the tungstate single crystal is stable in such a wide oxygen pressure range. In

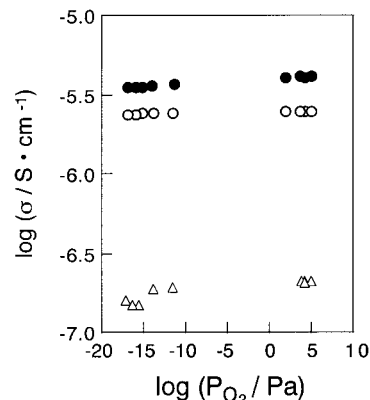


Figure 4. The oxygen pressure dependencies of the electrical conductivity for the single-crystal toward a -, b -, and c -axis directions in the oxygen pressure range from 10^{-18} to 10^5 Pa: ○, a -axis; ●, b -axis; △, c -axis.

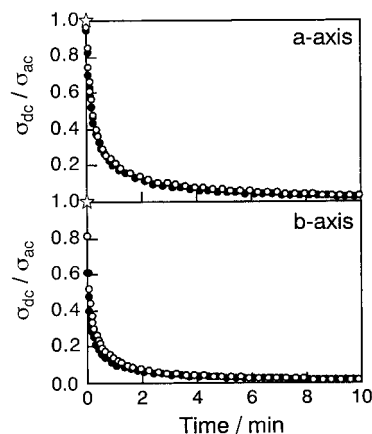


Figure 5. The time dependencies of the ratio of the dc to the ac conductivities (\star) at 700°C in oxygen (○) and in helium (●) for a $\text{Al}_2(\text{WO}_4)_3$ single crystal in the a - and b -axis directions, respectively.

addition to this, the constant conductivity means that electronic conduction is relatively unimportant and that $\text{Al}_2(\text{WO}_4)_3$ can be regarded as a nearly pure ionic conductor.

To investigate polarization effects in the electrical properties, the dc conductivity was measured as a function of time and compared with the ac data. Figure 5 shows the time dependencies of the ratio of the dc to the ac conductivities (\star) at 700°C in oxygen and in helium for a $\text{Al}_2(\text{WO}_4)_3$ single crystal in the a - and b -axis directions, respectively. The dc conductivities decrease with time abruptly in comparison with the ac values and approach a steady value for both directions. The steady-state dc conductivities obtained were about 2 orders of magnitude lower than the ac ones. From these polarization behaviors, the ionic transference number is approximately 0.99 for the $\text{Al}_2(\text{WO}_4)_3$ single crystal along both a - and b -axes and thus the single crystal is almost a pure ionic conductor, consistent with the results of the oxygen pressure studies. In contrast, for the c -axis, electrical conductivities obtained by both ac and dc are too low to identify the exact polarizing behavior.

The data of Figure 5 can also be used to investigate the possibility of O^{2-} conduction as the P_{O_2} values differ by a factor of $\sim 10^5$ between the oxygen and helium atmosphere (10^5 and 4 Pa). Note that the same

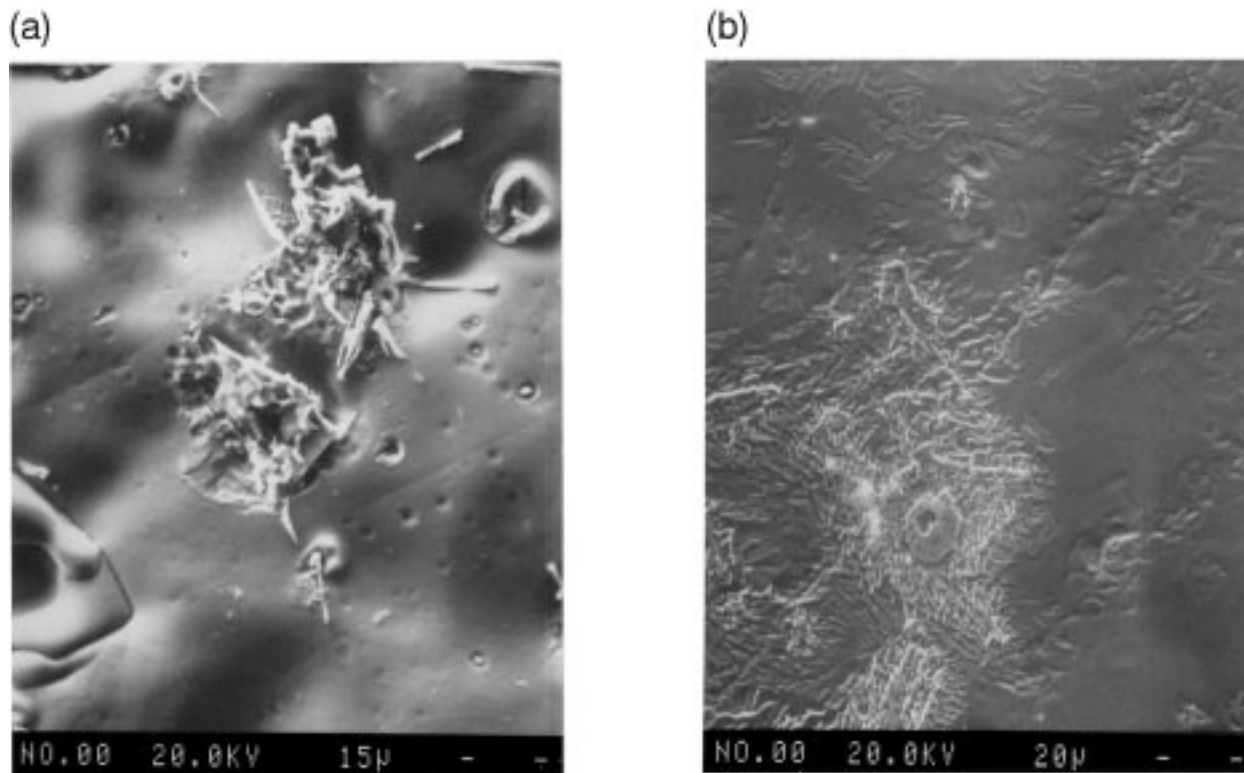


Figure 6. The photographs of the cathodic (a) and the anodic (b) surfaces of the $Al_2(WO_4)_3$ single crystal after the electrolysis.

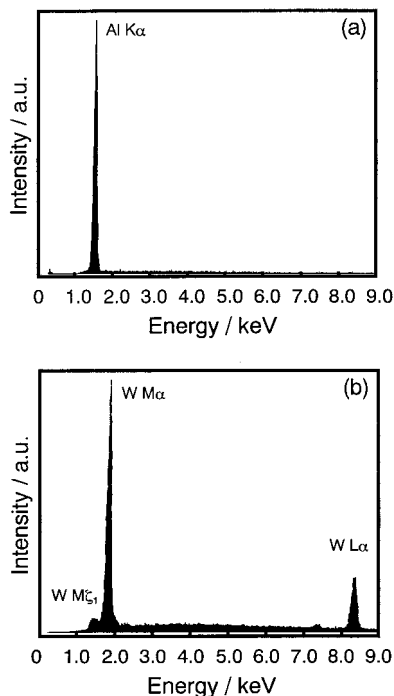


Figure 7. The spot analysis results obtained by the EPMA measurements for the deposits on the cathodic (a) and anodic (b) surface of the $Al_2(WO_4)_3$ single crystal after the electrolysis.

polarization behavior was seen in both atmosphere, i.e., a rapid decrease in the σ_{dc}/σ_{ac} ratio with increasing time. If O^{2-} is the predominant mobile ion species in the single crystal, a clear polarization would be expected in the helium atmosphere, while in the oxygen atmosphere no polarization should appear, as described in ref 13. The fact that the same polarization behavior is observed in Figure 5 clearly means that the oxide anion can be excluded as a candidate for the mobile ionic

species in $Al_2(WO_4)_3$ single crystals and, thus, that the mobile ions are cationic species.

Parts a and b of Figure 6 show the SEM photographs of the cathodic and the anodic surfaces of the $Al_2(WO_4)_3$ single crystal after electrolysis. In Figure 6a, the deposits were analyzed by EPMA measurements (Figure 7a) and only aluminum was found. In contrast, the substance appearing as a ring-like shape in Figure 6b was found to contain tungsten but not aluminum (Figure 7b). These results explicitly indicate that the Al^{3+} ion migrates from the anodic side to leave tungsten as tungsten oxide and that the migrating Al^{3+} ions deposit at the cathodic side as elemental aluminum and are instantly oxidized by oxygen in the ambient atmosphere.

From the results described above, the $Al_2(WO_4)_3$ single crystal has been clearly demonstrated to be a pure Al^{3+} ion conducting solid electrolyte with an anisotropic conducting behavior with a preferred *b*-axis direction.

Acknowledgment. The authors wish to express their thanks to Prof. H. Horiuchi for determining the axis directions and the lattice parameters of the single crystal by four-circle single crystal diffractometer. We also thank Dr. K. Yamada for the EPMA measurements. The present work was partially supported by a Grant-in-Aid for Scientific Research No. 09215223 on Priority Areas (No. 260), No. 06241106, 06241107, and 093065 from The Ministry of Education, Science, Sports and Culture. This work was also supported by the “Research for the Future, Preparation and Application of Newly Designed Solid Electrolytes (JSPS-RFTF96P00102)” Program from the Japan Society for the Promotion of Science.